Long-Term Characterization of the Boundary-Layer for Studying Land-Surface Atmosphere Interactions

Marke[1], T., S. Crewell[1], J. H. Schween[1], E. O'Connor[2], A. Manninen[3], U. Rascher[4] and M. Matveeva[4]

[1] Institute of Geophysics and Meteorology, University of Cologne, Germany, [2] Finnish Meteorological Institute, Finland, [3] University of Helsinki, Finland, [4] Forschungszentrum Jülich, Germany

JOYCE - CF

Graduate School of Geosciences

1. Jülich Observatory for Cloud Evolution (JOYCE)

- Location: Western Germany (50.9°N, 6.4°E)
- Continuous and highly-resolved boundary-layer (BL) measurements since 2011
- Ground based passive and active remote sensing and in-situ instruments
- Here: different approaches to characterize the atmospheric state are shown

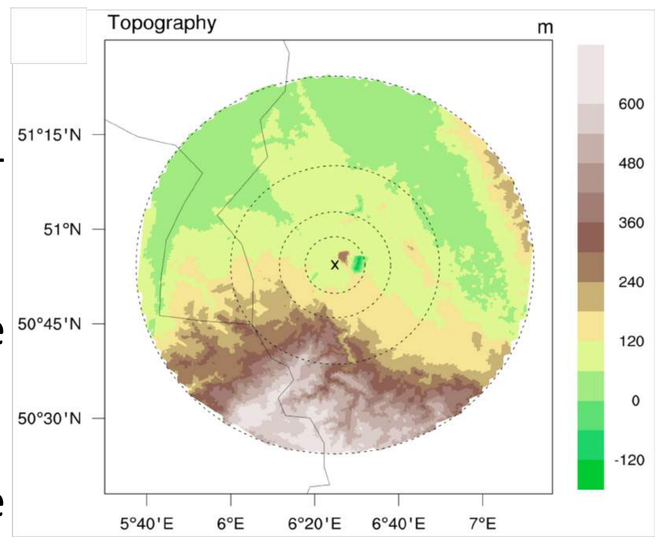

Fig. 1: Topographic map (height above m.s.l.) of the study area centered around JOYCE.

2. Boundary-Layer Classification with Doppler Lidar [1]

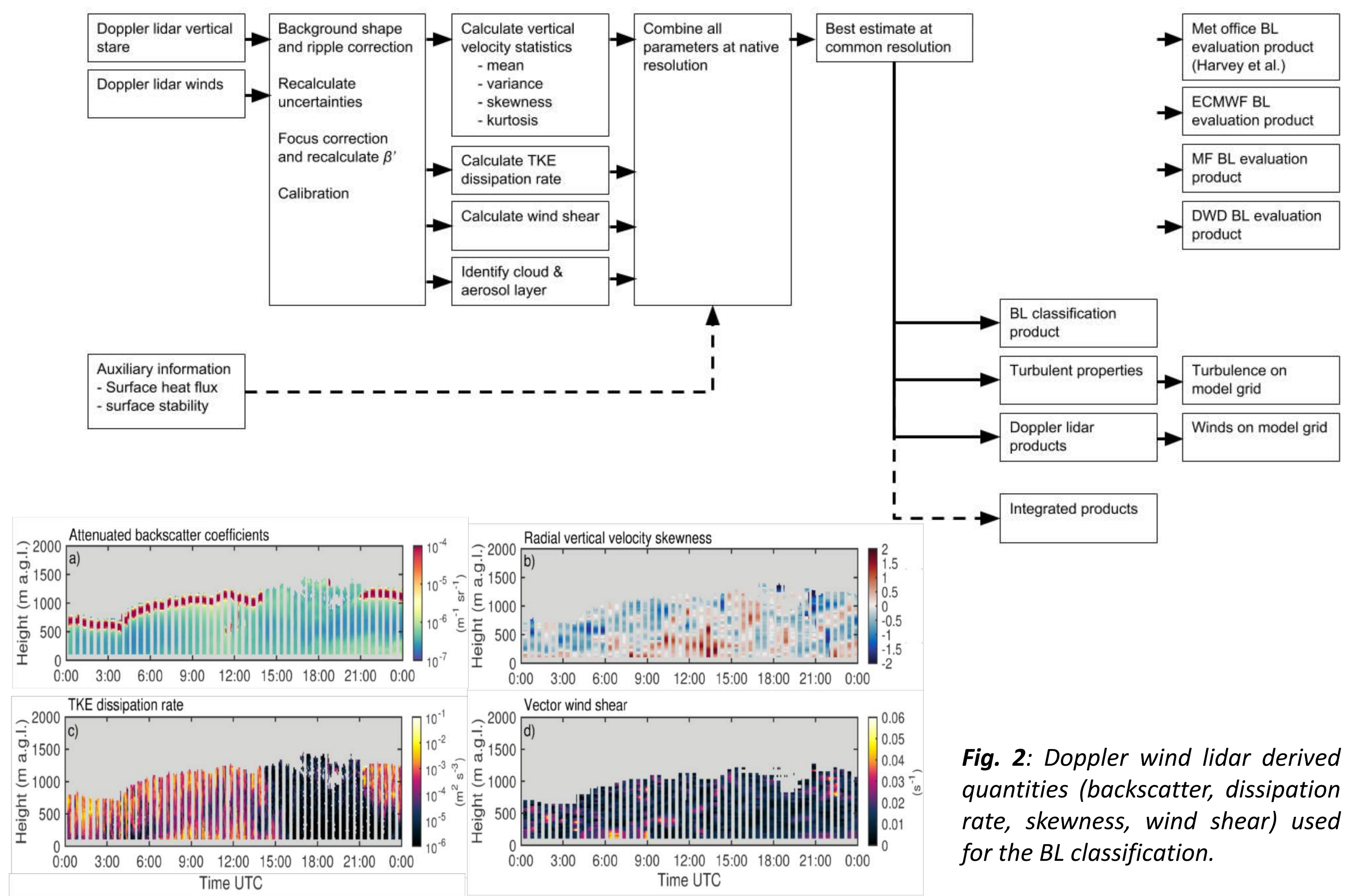

Fig. 2: Doppler wind lidar derived quantities (backscatter, dissipation rate, skewness, wind shear) used for the BL classification.

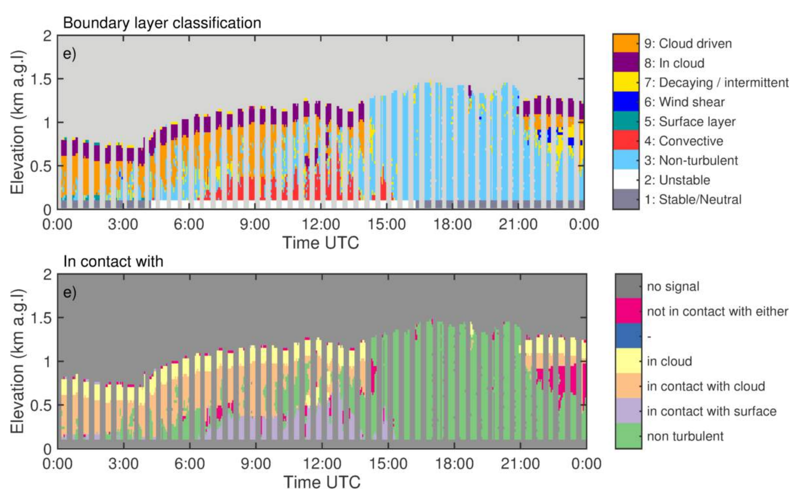

Fig. 3: Boundary-layer classification product with fields for describing the source of turbulence (top) and the connectivity of turbulence (bottom).

Doppler wind lidar (DWL) observations (Fig. 2) are used to derive a BL classification providing:

- Horizontal wind, turbulence
- Source of turbulence (Fig. 3)

Application to different sites for information on the diurnal and seasonal BL development

3. Low-Level Jet Climatology & Interactions with Topography [2]

Low-level jet (LLJ) importance:

- Evolution of clouds and precipitation
- Wind energy applications

Long-term DWL observations for:

- LLJ characteristics
- Diurnal/seasonal development

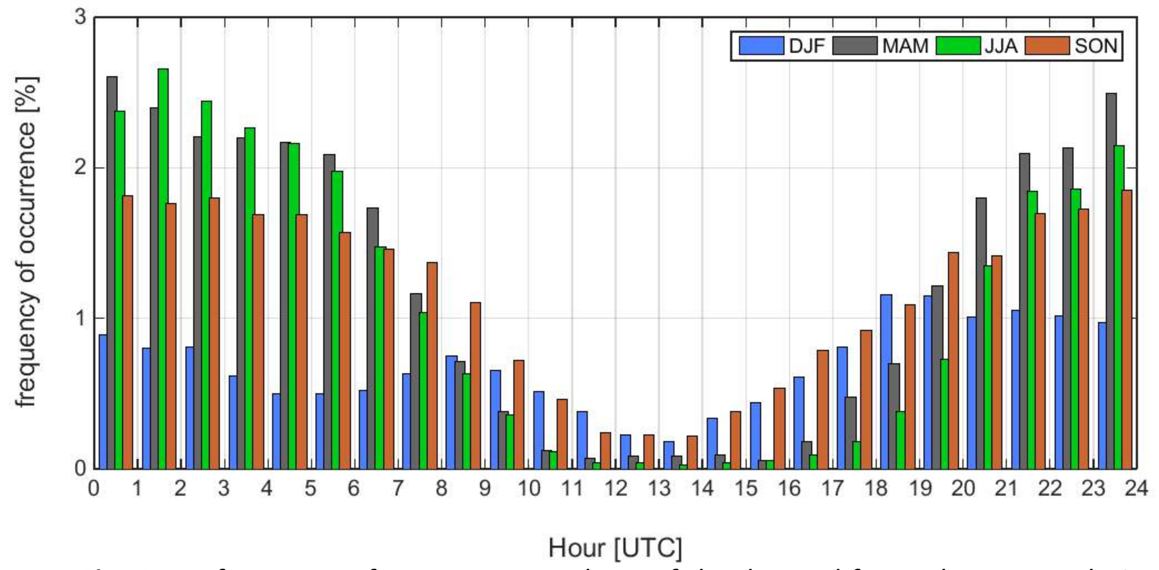

Fig. 4: LLJ frequency of occurrence per hour of the day and for each season relative to the total amount of detected LLJs at JOYCE.

- Common during nighttime (Fig. 4)
- Less pronounced diurnal cycle in DJF
- LLJ speed (height): 8.82 m/s (375 m)
- 15% below 200 m

	no-LLJ (4039 cases)	**LLJ** (698 cases)
LH	6.25 W m^{-2}	0.65 W m^{-2}
SH	-23.97 W m^{-2}	-11.73 W m^{-2}
NEE	0.94 μmol m^{-2} s^{-1}	0.74 μmol m^{-2} s^{-1}
u_*	0.18 m s^{-1}	0.11 m s^{-1}
z/L	0.06	0.16
σ_w	0.07 m s^{-1}	0.02 m s^{-1}
p_{air}	1006.61 hPa	1008.79 hPa
CO_2	401.2 ppm	411.6 ppm

***Table 1**: Median values of nighttime eddy-covariance tower measurements during DJF for LLJ and no-LLJ cases*

- Flux reduction due to lower troposphere decoupling (Table 1)
- Above surface layer: high wind shear and turbulence (Fig. 5)

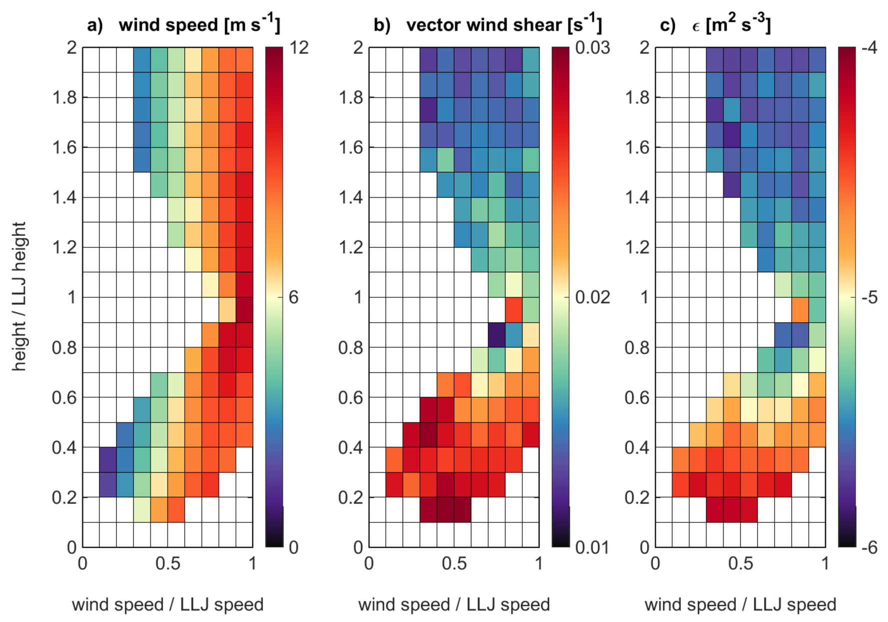

Fig. 5: Distribution of average wind speed (a), vector wind shear (b) and dissipation rate (c) as a function of normalized wind speed (abscissa) and height (ordinate) of the LLJ.

- Large-eddy simulations (LES) show an influence on the horizontal wind by scaling the topography
- Vertical velocity variations depend on wind direction (Fig. 6)

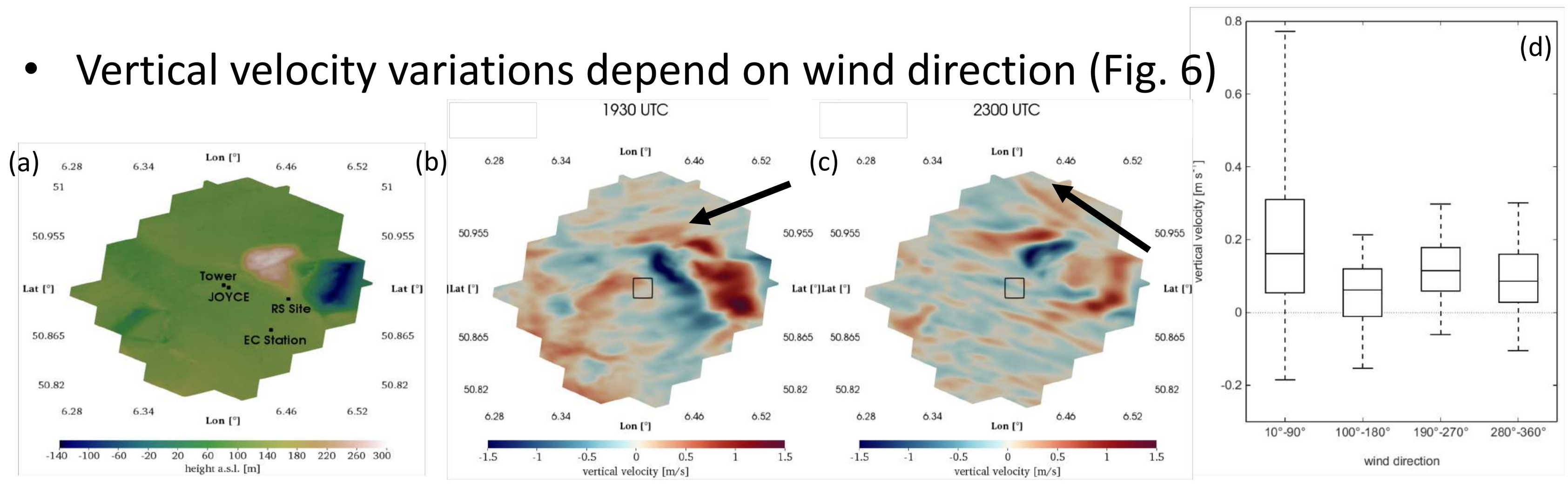

Fig. 6: ICON-LEM topographic map (10 km radius, 78 m horizontal resolution, [4]) centered around JOYCE (a). Simulated vertical velocity at 300 m a.s.l. on 2 May 2013 at 1930 UTC (b) and 2300 UTC (c). The black arrows denote the wind direction at 300 m. Vertical wind speed distributions measured by the wind lidar between 225 m and 705 m for different wind directions (d).

4. Water Vapor Patterns Connected to Land Surface Properties

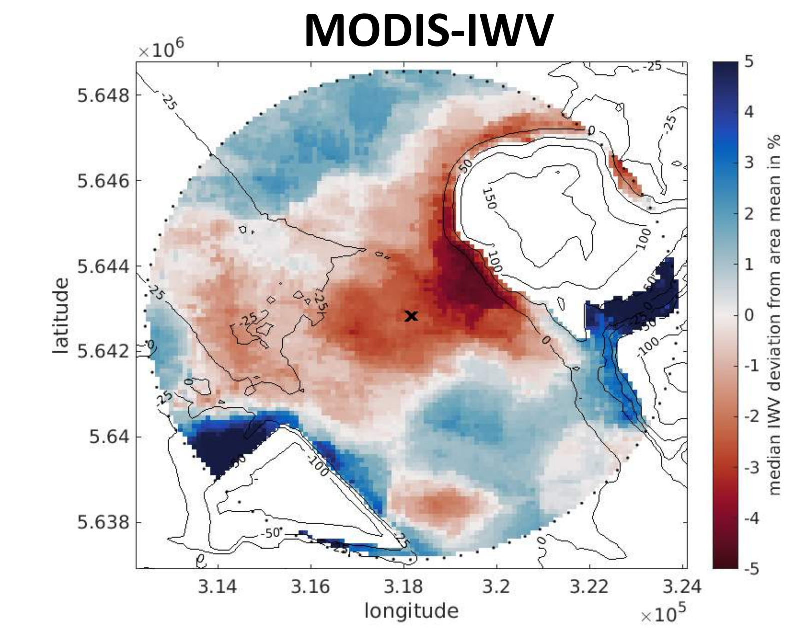

Fig. 7: Median values of the IWV deviation from the area mean (6 km radius) of the MODIS-NIR water vapor product (40 days).

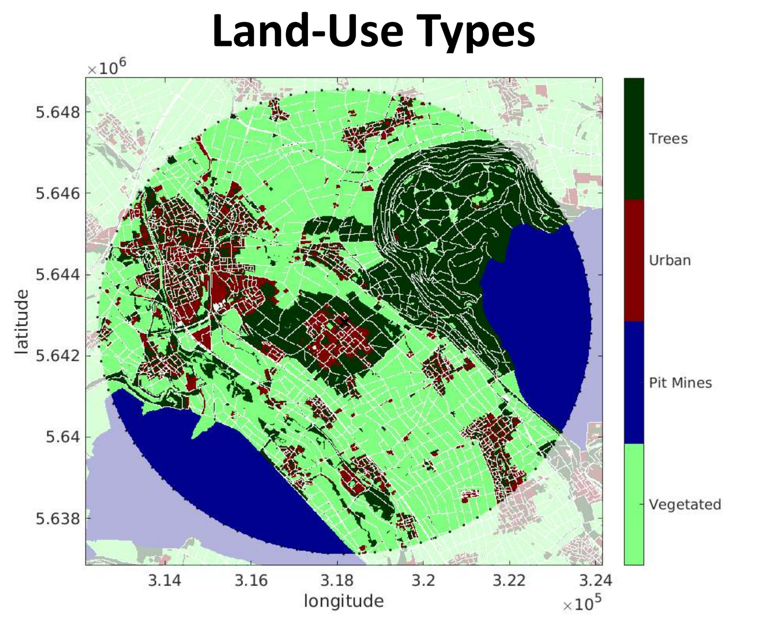

Fig. 8: Simplified land-use classification [3] using four types (vegetated, pit mines, forest, urban).

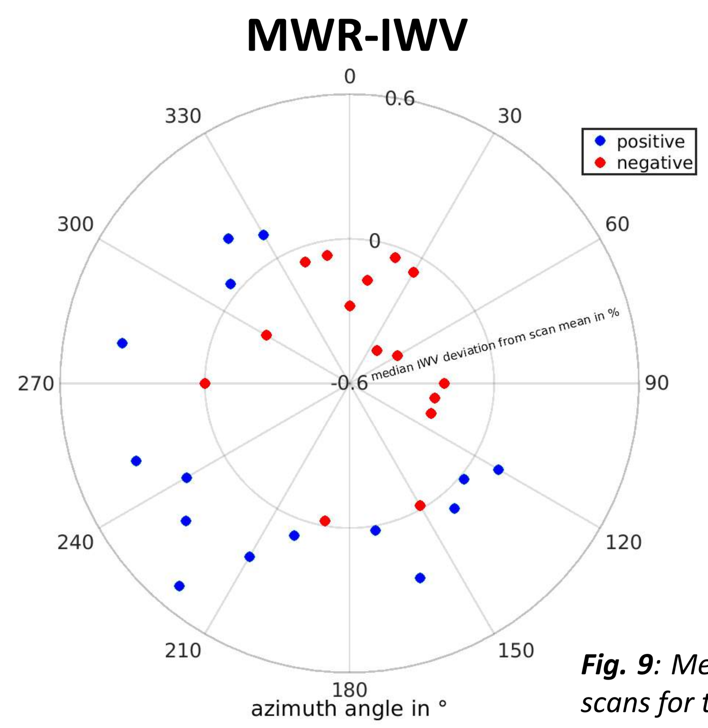

Fig. 9: Median values of the IWV deviation from the mean of the MWR scans for the times of the MODIS overpasses (9-14 UTC, 394 scans).

- MODIS NIR water vapor product used for investigating spatial patterns of integrated water vapor (IWV)
- Clear-sky periods are identified by Microwave Radiometer (MWR) scans at 30° elevation
- IWV deviations from the mean of the area (scan) of MODIS (MWR) show connections to the land-use (Fig. 7-9)

5. Outlook

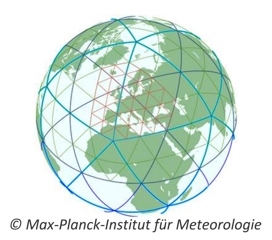

- Sensitivity study using LES with different settings regarding the surface properties

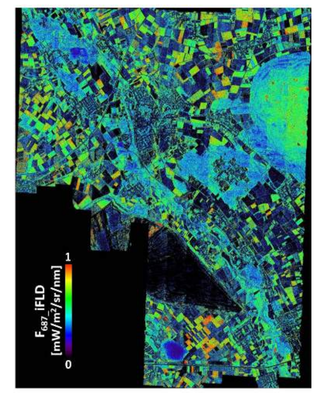

- High-resolution airborne imaging spectrometer (HyPlant, [5]) to connect IWV patterns to surface properties

References:

[1] Manninen, A., T. Marke, E. O'Connor, and M. Tuononen, 2018: Atmospheric boundary layer classification with Doppler lidar, *J. Geophys. Res.* , 123.

[2] Marke, T., S. Crewell, J. H. Schween, and M. Tuononen, 2018: Long-Term Observations and High Resolution Modeling of Mid-Latitude Nocturnal Boundary-Layer Processes Connected to Low-Level-Jets, *JAMC.*

[3] Waldhoff, G., Lussem, U., Bareth, G. (2017): *Multi-Data Approach for remote sensing-based regional crop rotation mapping: A case study for the Rur catchment, Germany. Int. J. Appl. Earth Obs. 61, 55-69.*

[4] Heinze, R. , et al. (2017): *Large-eddy simulations over Germany using ICON: a comprehensive evaluation. Q.J.R. Meteorol. Soc., 143: 69-100.*

[5] *Damm, A., Guanter, L., Laurent, V. C. E., Schaepman, M. E., Schickling, A., Rascher, U., 2014: FLD-based retrieval of sun-induced chlorophyll fluorescence from medium spectral resolution airborne spectroscopy data, Remote sensing of environment 147, 256 - 266 (2014)*

2018 AGU Fall Meeting, Washington D.C., USA, 10-14 Dec 2018

tmarke@meteo.uni-koeln.de

Grant: GSGS-2018X-02 Cologne Graduate School of Geosciences